the following identity[6]:

$$K_a{}^{b\alpha}D_{dc\beta}{}^{ab\alpha}=K_a{}^{c\beta}D_{db\alpha}{}^{ac\beta}.$$

Using Eq. (2), it is a straightforward calculation to obtain the expression of W. (We further use the approximation $\langle\omega^3\rangle/\langle\omega\rangle\approx\langle\omega^2\rangle$.) The expressions for D and W are given by Eqs. (1) and (3). However, in some of the D's and W's the "linear" approximation is not satisfied very well if we substitute the experimental masses using a reasonable cutoff. Since the Feynman integrals should go to zero if the masses of the virtual particles go to infinity (assuming smooth form factors), we modify the linear approximation by setting the values of the D's and the W's to be zeros if they turn out to be negative according to the linear approximation.

[6] R. E. Cutkosky and M. Leon, Phys. Rev. 138, B667 (1965).

PHYSICAL REVIEW VOLUME 151, NUMBER 4 25 NOVEMBER 1966

Phenomenological Analysis of $K^+\Lambda$ Photoproduction*

H. THOM
Laboratory of Nuclear Studies, Cornell University, Ithaca, New York
(Received 14 February 1966)

Low-energy $K\Lambda$ photoproduction cross-section and polarization data are analyzed using contributions from nonresonant perturbation amplitudes associated with p, K^+, Λ, Σ, and K^{*+} propagators, and from a resonant amplitude in one total and final orbital angular momentum state. The resonance is assumed to have an energy of about 1.7 GeV and a width of about 100 MeV. The data are analyzed by assuming that the resonance can be in any one of the angular momentum states from $S_{1/2}$ to $F_{5/2}$, and a χ^2 minimization is performed for each possibility. It is found that the perturbation amplitudes alone give good fits to the cross-section data, and that only a small amount of resonant amplitude in any one of a number of angular momentum states is sufficient to explain the polarization without strongly modifying the cross-section fits. The assumed resonant state in general contributes about 20% to the total cross section, and $P_{1/2}$ and $D_{3/2}$ states give the lowest values of χ^2. The values of the coupling constants obtained herein are compared with those expected from $SU(3)$; approximate agreement is found though the values obtained in our analysis are generally smaller than the $SU(3)$ predictions. The possible contribution of an $F_{5/2}$ resonant amplitude found in the analysis is consistent with that expected from $SU(3)$ for the third resonance. A compilation of all the presently existing $K\Lambda$ photoproduction data is given as an appendix.

I. INTRODUCTION

THIS paper reports the results of a systematic phenomenological analysis of the reaction $\gamma+p\rightarrow K^++\Lambda$ in the total c.m. energy region from 1.61 GeV (threshold) to 1.82 GeV. The model used in the analysis is similar or identical to models used previously by many authors[1–5] in photoproduction analysis. In the absence of a complete theory for reactions in this energy region, second-order perturbation theory is used to determine all the nonresonant partial-wave amplitudes.[6] In order to account for the experimentally observed Λ polarization, it is then assumed that one particular J,l state (total and final orbital angular momentum, respectively) is resonant at a total energy of about 1.7 GeV. The contribution of this state is represented by a basically nonrelativistic Breit-Wigner amplitude, and two assumptions are then considered: either the resononance is entered through a pure electric or magnetic multipole, or it is entered through a mixture of the two. Resonant amplitudes are considered in all states from $S_{1/2}$ through $F_{5/2}$. In calculating the nonresonant amplitudes, the unknown coupling constants and magnetic moments of perturbation theory are treated as adjustable parameters. For the resonant amplitude, the total and partial widths, and the resonant energy are considered as adjustable parameters. The fit of the calculations to the experimental data is optimized by an iterative procedure which minimizes χ^2. This is done by a gradient search and quadratic fit of χ^2 in the space of the adjustable parameters. A number of reasonably good fits to the experimental data are found for different resonant states, so there is no conclusive evidence that a particular resonance is strongly favored, though $D_{3/2}$ and $P_{1/2}$ resonances give the best fits. Optimum coupling constants and magnetic moments differ somewhat for the various resonance assumptions, and some feeling can be gained of their sensitivity in this model.

The general features of the experimental data of the photoproduction process and of the parallel $\pi^-+p\rightarrow K^0+\Lambda$ reaction give at least an intuitive basis for the

* Supported in part by the National Science Foundation.
[1] S. Hatsukade and H. J. Schnitzer, Phys. Rev. 128, 468 (1962); 132, 1301 (1963); S. Hatsukade, L. K. Pandit, and A. H. Zimerman, Nuovo Cimento 34, 819 (1964).
[2] M. Gourdin and J. Dufour, Nuovo Cimento 27, 1410 (1963); J. Dufour, *ibid.* 34, 645 (1964); 35, 860 (1965).
[3] N. A. Beauchamp and W. G. Holladay, Phys. Rev. 131, 2719 (1963).
[4] T. K. Kuo, Phys. Rev. 129, 2264 (1963); 130, 1537 (1963).
[5] Fayyazuddin, Phys. Rev. 123, 1882 (1961); 134, B182 (1964).
[6] This use of "perturbation theory" can be partially justified. See M. Cini and S. Fubini, Ann. Phys. (N. Y.) 3, 352 (1960).

simple phenomenological model used. Though these features are discussed elsewhere,[4,7,8] it is worth mentioning them here.

Measurements of the photoproduction differential cross section[9–11] now exist for incident laboratory photon energies (E_γ) from 0.934 to 1.400 GeV.[12] Over this energy range the angular distributions ($d\sigma/d\Omega$) show remarkably little change. The cross section is peaked at forward K angles; the amount of peaking increases slowly from threshold to 1.2 GeV and then appears to drop slightly between 1.2 and 1.4 GeV.[13] An estimate of the integral cross section from the differential data indicates that $\sigma \approx 2.2$ μb from 1.0 to 1.4 GeV.

The Λ polarization has been measured at about 90° in the $K\Lambda$ c.m. system over a photon energy range of 0.960 to 1.300 GeV.[14–16] It is appreciable in the region from 1.0 to 1.2 GeV (of the order of 30% in the direction $\hat{p}_\gamma \times \hat{p}_\Lambda$) and there is some indication that it is dropping toward zero at 1.3 GeV.

From a consideration of the $K\Lambda$ photoproduction alone, it is clear that there is very little justification for assuming a resonance at a total energy of 1.7 GeV. The integral cross section shows no enhancement at the assumed resonant energy. The differential cross section shows no classic sign reversal of interference terms above and below the suspected energy. Only the polarization indicates the necessity for anything but perturbation-type amplitudes. Bearing in mind the fact that perturbation theory gives real partial-wave amplitudes which are only slowly varying functions of energy, it is likely that the excitation curve of the polarization should approximately mirror that of the imaginary amplitude causing it. The statistical errors of the polarization measurements are very large, but the data do suggest a shape like the imaginary part of a resonant amplitude centered around 1.05-GeV photon energy.

The strong parallel between πN elastic scattering and πN photoproduction suggests the usefulness of looking at the data of the reaction $\pi^- + p \rightarrow K^0 + \Lambda$. Though there are some basic inconsistencies in the results of different experiments, the integral cross section shows a pronounced bump at a total energy of 1.7 GeV with a width of about 100 MeV (full width at half-maximum) and the polarization is very large (in some cases near 100%). At the present time, the angular momentum and parity of this resonance in the $\pi p \rightarrow K\Lambda$ system has not been undisputably determined though it appears likely that it is a $P_{1/2}$ state.[7,17] The problem of determination arises largely because the data above 1.7 GeV are scarce so there is no proof that the bump is caused by a resonance in the usual sense.[7] It is this apparent resonance in the (πp,$K\Lambda$) system which really leads us, by analogy with πp photoproduction, to use a resonant partial-wave amplitude in $K\Lambda$ photoproduction. The quantum numbers of this resonance are assumed to be unknown in this calculation in order to ascertain if photoproduction can yield a convincing choice of its own.

The basic phenomena of the πp ($T=\frac{1}{2}$) system should also be kept in mind (the $K\Lambda$ system is pure $T=\frac{1}{2}$), although only the $F_{5/2}$, third resonance, is considered explicitly in this model. The third resonance has a mass of 1.688 GeV and could well decay into the $K\Lambda$ system, though the centrifugal barrier is very strong. Dufour[2] has already found reasonable agreement with the low-energy (γp,$K\Lambda$) data using such a resonance.[18] The second πN resonance ($D_{3/2}$, 1.518 GeV) could have an effect as a background amplitude but has been ignored as has the more recently discovered $P_{1/2}$ (1.500-GeV) resonance.[19]

II. PHENOMENOLOGICAL MODEL

A. Nonresonant Amplitudes

Figure 1 shows the Feynman diagrams which are associated with the perturbation amplitudes used in this paper. These consist of the standard Born terms and the vector meson (K^*, 891 MeV) exchange term.

[7] G. T. Hoff, Phys. Rev. **139**, B671 (1965); Phys. Rev. Letters **12**, 652 (1964); Phys. Rev. **131**, 1302 (1963).

[8] H. Uto, L. B. Auerbach, K. Lande, A. K. Mann, F. J. Sciulli, D. H. White, and K. K. Young, Bull. Am. Phys. Soc. **10**, 466 (1965); Hiroaki Uto, thesis, University of Pennsylvania, 1965 (unpublished).

[9] R. L. Anderson *et al.*, Phys. Rev. Letters **9**, 131 (1962).

[10] C. W. Peck, Phys. Rev. **135**, B830 (1964).

[11] R. L. Anderson *et al.*, paper presented at The International Symposium on Electron and Photon Interactions at High Energies, Hamburg, 1965 (unpublished); N. Stanton, thesis, Cornell University, 1965 (unpublished).

[12] See Table III in Appendix I for conversions to c.m. energies and equivalent laboratory pion energies.

[13] Data at very forward angles exist only for the 1.2- and 1.4-GeV energies. The 1.2-GeV data were measured at the California Institute of Technology, whereas the 1.4-GeV data were measured at Cornell University, so there is a possibility of systematic differences. In this paper the 1.4-GeV data have not been used in obtaining the χ^2 fits. The model with only one resonance at about 1.05 GeV (E_γ) is not likely to be applicable at 1.4 GeV, where other resonances may be more influential.

[14] H. Thom *et al.*, Phys. Rev. Letters **11**, 433 (1963).

[15] B. Borgia *et al.*, Nuovo Cimento **32**, 218 (1964); M. Grilli *et al.*, *ibid.* **38**, 1467 (1965). These authors also have one polarization point at a K c.m. scattering angle of 61°. This measurement has been ignored in our χ^2 analysis, although it is compared with some of the fits.

[16] D. E. Groom and J. H. Marshall (to be published). The final results of Groom and Marshall are quoted in Appendix II. D. E. Groom and J. H. Marshall, paper presented at the International Conference on High Energy Physics, Moscow, 1964 (unpublished). Data given at this conference were preliminary.

[17] The possibility of a $P_{1/2}$ or $P_{3/2}$ resonance was originally proposed by A. Kanazawa, Phys. Rev. **123**, 997 (1961).

[18] G. T. Hoff (Ref. 7) uses a very narrow ($\Gamma \approx 9$ MeV) $F_{5/2}$ resonance at 1.647 GeV (distinct from N^{***}) in her (πp,$K\Lambda$) analysis. The need for the existence of this resonance is based on the old experimental data of L. Bertanza *et al.*, Phys. Rev. Letters **8**, 332 (1962), which indicate a change in the sign of the polarization as a function of angle at $T_\pi = 929$ MeV. The recent experimental data of H. Uto *et al.* (Ref. 8) indicate no change in the sign of the polarization in the momentum range $950 \leq p_\pi \leq 975$ MeV/c. Thus the existence of this resonance is quite unlikely and it will be ignored throughout this paper.

[19] See for example, L. D. Roper *et al.*, Phys. Rev. **138**, B190 (1965). Results from proton-proton inelastic scattering (F. Turkot, private communication) indicate a lower resonant energy of 1.4 GeV.

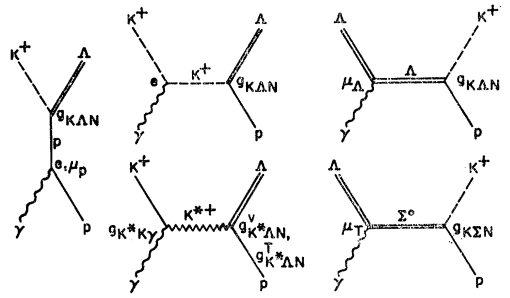

FIG. 1. Feynman diagrams for the perturbation amplitudes which give the nonresonant background for all models considered here.

Both vector and tensor coupling of the K^* to the baryon are included. Derivations of the amplitudes resulting from the Born terms[20] of Fig. 1 have been given in many places,[1,2,4] so only explicit definitions of the coupling constants or vertex factors, along with the final results, are given in Appendix I. Of the nine coupling constants which appear, only e and μ_p are known, and μ_Λ is approximately known.[21] Throughout these calculations we have used $\mu_\Lambda=-1.0\ e/2M_\Lambda$. This is approximately halfway between the measured value of $-0.73\pm0.17\ e/2M_p$ and the predicted $SU(3)$ value of $-0.95\ e/2M_p$. Any error in μ_Λ is absorbed into the Λ, Σ transition moment (μ_T) without loss of generality.[22] The remaining six coupling constants are unknown but some of them can be lumped into pairs, leading to four adjustable parameters defined as follows:

$$\begin{aligned} g_\Lambda &= g_{K\Lambda N}, \\ G_\Sigma &= \kappa_T g_{K\Sigma N}, \\ G_V &= g_{K^*K\gamma} g^V{}_{K^*\Lambda N}, \\ G_T &= g_{K^*K\gamma} g^T{}_{K^*\Lambda N}, \end{aligned} \tag{1}$$

where κ_T is defined by

$$\mu_T=\kappa_T e/(M_\Lambda+M_\Sigma).$$

The Born amplitudes can be expanded into a sum of partial-wave amplitudes, $E_{l\pm}$ and $M_{l\pm}$.[23] This expansion is desirable because it gives not only the relative importance of the various nonresonant amplitudes but also a comparison between the resonant amplitude of a particular l,J state and the Born amplitude it is modifying. The resulting partial-wave fits to the data can be looked upon by the skeptic as kinematically reasonable fits[24] which may be of more basic significance than the model used to generate them. Over the energy region of interest it is found that expansions through $F_{5/2}$ are sufficient to reproduce exact Born amplitudes accurately.

For reasons of expediency, a number of possible phenomena have been disregarded by considering only the diagrams of Fig. 1. The Y_1^* and Y_0^* (1383 and 1405) exchange diagrams have not been considered though the propagators for these resonances are not significantly smaller than that of the Σ, and recent measurements have found a non-negligible cross section for Y^* photoproduction near threshold.[25] Secondly, if one looks upon our analysis as some sort of approximation to a dispersion relation calculation, then one is ignoring all the integral terms except the one which leads to the assumed resonant state. In this way all the resonances of the πN, $T=\frac{1}{2}$ system are ignored unless one of them corresponds to the phenomenological resonance; moreover, all effects of other channels opening are excluded. The fact that the diagrams of Fig. 1 give reasonable fits to the cross-section data hopefully implies that the above-mentioned phenomena do not have large effect. Finally, because many channels are open and four momentum transfers are large, absorption corrections and form factors may be appropriate if one considers the contributions from the diagrams of Fig. 1 in the spirit of phenomenological peripheral production models.[26]

B. Resonant Amplitudes

The partial-wave amplitudes for the resonant states are given a Breit-Wigner form.[27,28] Electric and magnetic transition amplitudes to states of l, $J=l\pm\frac{1}{2}$ (denoted by $l\pm$), where l is the final meson angular momentum and the J the total angular momentum, are

$$E_{l\pm(\mathrm{res})}=[qkj_\gamma(j_\gamma+1)]^{-1/2}\frac{W_0(\Gamma_E\Gamma_{l\pm})^{1/2}}{W_0{}^2-W^2-i\Gamma W_0},$$

where $j_\gamma=l\pm1$ and

$$M_{l\pm(\mathrm{res})}=[qkj_\gamma(j_\gamma+1)]^{-1/2}\frac{W_0(\Gamma_M\Gamma_{l\pm})^{1/2}}{W_0{}^2-W^2-i\Gamma W_0}, \tag{2}$$

where $j_\gamma=l$. Here W_0 and Γ are the mass and total width at half maximum of the resonance; q and k are the c.m. momentum of the K meson and photon, respectively, W is the total c.m. energy, j_γ is the photon angular

[20] Hereafter, the expression "Born terms" is used to describe all diagrams of Fig. 1.

[21] D. A. Hill *et al.*, Phys. Rev. Letters **15**, 85 (1965).

[22] Note that the only difference in the Λ and Σ exchange diagrams of Fig. 1 (except for the different coupling constants) is the small kinematical difference of the propagators $(\gamma\cdot p-M_\Lambda)^{-1}$ and $(\gamma\cdot p-M_\Sigma)^{-1}$. To a good approximation, the two diagrams could be treated as a single diagram with a composite coupling of $g_{K\Lambda N}\mu_\Lambda+g_{K\Sigma N}\mu_T$. See R. H. Capps, Phys. Rev. **114**, 920 (1959). Most of the fits of Dufour (Ref. 2) for different μ_Λ values are related in the above fashion, i.e., the value of $\mu_\Lambda+(g_{K\Sigma N}/g_{K\Lambda N})\mu_T$ is nearly constant for $\mu_\Lambda=-0.95$, -1.5, -1.91 $(e/2M_p)$.

[23] The amplitudes $E_{l\pm}$ and $M_{l\pm}$ refer to electric and magnetic transitions to states of final and total angular momentum l and $J=l\pm\frac{1}{2}$. See Appendix I and Ref. 60 for the expansion formulas.

[24] By this we mean that the nonresonant amplitudes have proper threshold behavior and are smoothly varying functions of energy. The resonant amplitudes have proper threshold behavior and also have real and imaginary parts which are related in the usual sense. See Ref. 19 for a discussion of partial-wave fitting. M. Rimpault, Nuovo Cimento **31**, 56 (1964), gives partial-wave fits to $\pi p\to K\Lambda$ which do not follow these rules and consequently are rather implausible.

[25] S. Mori, thesis, Cornell University, 1966 (unpublished).

[26] J. D. Jackson, Rev. Mod. Phys. **37**, 484 (1965).

[27] J. M. Blatt and V. F. Weisskopf, *Theoretical Nuclear Physics* (John Wiley & Sons, Inc., New York, 1952).

[28] For a recent discussion see J. D. Jackson, Nuovo Cimento **34**, 1644 (1964).

momentum. The partial decay widths of the resonance into the (γp) system are Γ_E or Γ_M, and $\Gamma_{l\pm}$ denotes the corresponding quantity for decay into the $(K\Lambda)$ system. The term $[qkj_\gamma(j_\gamma+1)]^{-1/2}$ is a normalization factor chosen so that the definition of $E_{l\pm}$ and $M_{l\pm}$ is consistent with the unitarity condition. The maximum possible contribution of a particular multipole amplitude, either $E_{l\pm}$ or $M_{l\pm}$, to the integral cross section is[29]

$$\sigma(E_{l\pm},M_{l\pm})=(\pi/4k^2)(2J+1).$$

The decay widths are in general momentum-dependent. Each is usually written in terms of a reduced width γ and a barrier penetration factor v_l. The general form is

$$\Gamma_l(q)=qRv_l(qR)\gamma, \tag{3}$$

where

$$v_l(qR)\propto(qR)^{2l} \quad \text{for} \quad qR\ll 1,$$

and

$$v_l(qR)\approx 1 \quad \text{for} \quad qR\gg 1.$$

Here q is the c.m. momentum of the decay particle and R is the interaction radius, which has been fixed at about one fermi ($1/R=200$ MeV) throughout these calculations.[30]

The total width Γ in Eq. (2) is assumed constant for lack of any information as to the dominant channel. Probably Γ is slowly varying compared with $(W_0^2-W^2)$. The partial decay width into the $K\Lambda$ system will be extremely momentum-dependent. Here the barrier penetration factors of nuclear physics[27] have been used in our calculations. [The exact expressions can be found in Appendix I, Eqs. (A12).] If one defines $\Gamma_{l\pm}{}^0$, $v_l{}^0(qR)$, q^0, and k^0 as the decay width, penetration factor, and momenta evaluated at W_0 then

$$\Gamma_{l\pm}=(q/q^0)[v_l(qR)/v_l{}^0(qR)]\Gamma^0{}_{l\pm}. \tag{4}$$

The c.m. momentum of the photon is large ($k\approx 0.6$ GeV) and only slowly varying so $v_l(kR)\approx 1$ and Γ_E (with a similar expression for Γ_M) can be approximated by

$$\Gamma_E=(k/k^0)\Gamma^0{}_E. \tag{5}$$

Equations (2) can be rewritten using Eqs. (4) and (5), and lead to

$$E_{l\pm(\mathrm{res})}=[q^0k^0j_\gamma(j_\gamma+1)]^{-1/2}\left[\frac{v_l(qR)}{v_l{}^0(qR)}\right]^{1/2}\times\frac{W_0\Gamma^0{}_{El\pm}}{W_0^2-W^2-i\Gamma W_0},$$
$$M_{l\pm(\mathrm{res})}=[q^0k^0j_\gamma(j_\gamma+1)]^{-1/2}\left[\frac{v_l(qR)}{v^0{}_l(qR)}\right]^{1/2}\times\frac{W_0\Gamma^0{}_{Ml\pm}}{W_0^2-W^2-i\Gamma W_0}, \tag{6}$$

where

$$\Gamma^0{}_{El\pm}=(\Gamma^0{}_E\Gamma^0{}_{l\pm})^{1/2}$$

and similarly for $\Gamma^0{}_{Ml\pm}$. The adjustable parameters for the resonant amplitudes are then W_0, Γ, $\Gamma^0{}_{El\pm}$, and $\Gamma^0{}_{Ml\pm}$.

Because of the large photon momentum involved in the reaction there is basically no kinematical reason for a resonant state to result from either a pure electric or a pure magnetic multipole. Therefore, resonant amplitudes which contain both electric and magnetic transitions to a particular J,l state are considered as well as the pure transitions.[31]

The resonant amplitudes must be combined with the nonresonant Born amplitudes. The lack of a theoretical model leaves much uncertainty in the manner in which this should be done.[32] The usual procedure is just to add the resonant multipole amplitude $E_{l\pm(\mathrm{res})}$ or $M_{l\pm(\mathrm{res})}$ to its nonresonant counterpart $E_{l\pm(\mathrm{non})}$ or $M_{l\pm(\mathrm{non})}$. However, if the Born amplitude is approximately the same size as the resonant amplitude, one wonders if the resultant sum has much to do with resonant behavior.

In our analysis we have checked the sensitivity of the calculations to the way in which the resonant and nonresonant terms are combined by using three forms for the resonant state amplitude. For $E_{l\pm}$ these are

$$E_{l\pm(\mathrm{tot})}=E_{l\pm(\mathrm{res})}, \tag{7a}$$
$$E_{l\pm(\mathrm{tot})}=E_{l\pm(\mathrm{non})}+E_{l\pm(\mathrm{res})}, \tag{7b}$$
$$E_{l\pm(\mathrm{tot})}=E_{l\pm(\mathrm{non})}\cos\delta e^{i\delta}+E_{l\pm(\mathrm{res})}, \tag{7c}$$

where

$$\cos\delta e^{i\delta}=(W_0^2-W^2)/(W_0^2-W^2-iW_0\Gamma).$$

Corresponding forms are used for $M_{l\pm}$.

In general the initial fits for a particular resonant state are performed using Eq. (7a) and then some of the more successful fits are recalculated using Eqs. (7b) and (7c). Fits for an S-wave resonance are attempted using only Eq. (7b). It is found that the various forms of Eq. (7) have little effect on most of the fits. (The $P_{3/2}$ resonant state is the only exception.)

The expressions for the resonant state amplitudes, Eqs. (7a) and (7c), are modeled after the general solution of the "Omnes equation" [33] and the results of dispersion calculations at low energy.[34,35] The solution of the dispersion integral equation in these calculations

[29] The dependence of the cross section of $E_{l\pm}$ and $M_{l\pm}$ is given in Appendix I.

[30] This is the standard choice though there is no strong justification for it. For another value see S. L. Glashow and A. H. Rosenfeld, Phys. Rev. Letters **10**, 192 (1963), and Ref. 42.

[31] When discussing resonant amplitudes which are both electric and magnetic transitions the mixture will be denoted by "$E_{l\pm}+M_{l\pm}$" where the "+" does not indicate simple addition of the multipole amplitudes but a combination through the use of Eqs. (3.8)–(3.11) of Ref. 60.

[32] The author is indebted to Professor P. Carruthers for pointing out the possible combinations considered here.

[33] R. Omnes, Nuovo Cimento **8**, 316 (1958). For an application to inelastic πN scattering, see P. Carruthers, Ann. Phys. (N. Y.) **14**, 229 (1961).

[34] G. F. Chew and F. E. Low, Phys. Rev. **101**, 1579 (1956).

[35] G. F. Chew, M. L. Goldberger, F. E. Low, and Y. Nambu, Phys. Rev. **106**, 1345 (1957); G. Höhler and W. Schmidt, Ann. Phys. (N. Y.) **28**, 34 (1964).

gives a resonant state amplitude in which resonant behavior is generated by multiplying at least part of the Born amplitude by a term proportional to $e^{i\delta}\sin\delta$, where δ is the elastic scattering phase shift. It is also found that part of the Born amplitude may be multiplied by a term proportional to $e^{i\delta}\cos\delta$ and consequently is diminished in the resonance energy region.

III. COMPUTATIONAL PROCEDURE

A. Data

The differential cross-section data of Refs. 9, 10, 11, 16, and 25 are tabulated in Table IV for easy reference. Some 46 data points for photon energies between 934 and 1200 MeV are used in the χ^2 fitting. These points are used without modification except for the one point at 934 MeV. It is found that this point is hard to fit no matter which model is used. Typically, the discrepancy is about three to five standard deviations; if this point is included in the χ^2 calculation without modification it tends to unduly influence the χ^2 value. For this reason it has been given an error three times its experimental statistical value.[36]

The polarization data given in Refs. 14, 15, and 16 are modified extensively to make the computations easier. It is assumed that all the points are measured at 90° c.m., and some of the points are interpolated to slightly different photon energies. This rather liberal interpolation is justified by the poor statistics of the polarization data. Table V gives the experimental data and the interpolated data used in the χ^2 determination.[37]

B. χ^2 Optimization

The fits to the data are optimized by minimizing the quantity

$$C^2=\chi_\sigma{}^2+2\chi_P{}^2,$$

where

$$\chi_\sigma{}^2=\sum_{i=1}^{46}\left[\frac{\sigma_i(\text{expt})-\sigma_i(\text{cal})}{\Delta\sigma_i(\text{expt})}\right]^2$$

and

$$\chi_P{}^2=\sum_{i=1}^{8}\left[\frac{P_i\sigma_i(\text{expt})-P_i\sigma_i(\text{cal})}{\Delta P_i\sigma_i(\text{expt})}\right]^2. \tag{8}$$

In these expressions, σ_i(expt) and $\Delta\sigma_i$(expt) are the experimental differential cross sections and experimental errors in the cross sections, and σ_i(cal) is the calculated cross section; $P_i\sigma_i$(expt), $\Delta P_i\sigma_i$(expt), and $P_i\sigma_i$(cal) are the same quantities for the product of the differential cross section and the polarization. The arbitrary weighting factor of 2 in C^2 is chosen so as to ensure good fits to the polarization.

The χ^2 divided by the number of degrees of freedom N is given in Tables I and II. In fits which involve resonant amplitudes, for which both cross-section and polarization data are used, χ^2/N is defined by

$$\chi^2/N=(\chi_\sigma{}^2+\chi_P{}^2)/N, \tag{9a}$$

where N is 46 or 47 depending on whether a resonant amplitude is assumed to come from both $E_{l\pm}$ and $M_{l\pm}$ or from just one of them. When the cross-section data alone are fit by just Born amplitudes, χ^2/N is defined by

$$\chi^2/N=\chi_\sigma{}^2/N, \tag{9b}$$

where N is 42. Though Born terms alone yield zero polarization, the cross-section fits derived from them are useful in determining whether the addition of a resonant amplitude significantly improves the fits.

The technique for finding parameters which optimize C^2 is a rather straightforward computer gradient search procedure.[38] Initially, W_0 and Γ are set at 1.7 GeV and 100 MeV, respectively, and held fixed. The other five or six parameters (g_Λ, G_Σ, G_V, G_T, $\Gamma^0{}_{El\pm}$, $\Gamma^0{}_{Ml\pm}$) are chosen randomly from within a suitable range of values. Then C^2 is computed and the rate of change of C^2 with each parameter found. The values of the parameters are then changed so as to move C^2 a certain distance along the direction of its gradient. A new C^2 is computed and if it is smaller than the previous one, more steps are taken in the same direction until C^2 no longer decreases. At this point a new gradient is calculated and the procedure is repeated. If C^2 is increased on the first step, a parabola is fit to C^2 as a function of the parameters and C^2 is recalculated at the minimum of the parabola. It is found convenient to have scale factors associated with the parameters so that their relative sensitivity and step sizes can be varied. At various stages in the calculation, C^2 is tested to see if it is reasonably small and is improving rapidly enough to make continuing the calculation worthwhile. If the behavior of C^2 is not promising, new arbitrary parameters are chosen and the calculation is started over. If small values of C^2 are obtained, W_0 and Γ are allowed to vary in order to optimize C^2 still further. For each type of resonant amplitude, about twenty initial choices are traced through the optimization procedure. Some of the most successful fits are given in Table I. We would stress that a smaller value of C^2 for one resonant state as compared with another does not mean that the first state definitely provides a better fit; it only says that a better solution for the second state has not been found.

IV. RESULTS

Table I lists some of the most successful values of the parameters for fits to just Born amplitudes and for fits incorporating the various resonance assumptions. All

[36] Two new low-energy points measured by S. Mori (Ref. 25) seem to be consistent with this 934 point so perhaps the modification is unjustified. More low-energy measurements may point up the need for a modification of our model.

[37] The newer data of Ref. 15 were not available at the time the calculations were carried out.

[38] The author is indebted to R. Reid from whose more sophisticated techniques came the methods and ideas incorporated in this procedure.

TABLE I. Characteristic values of the parameters of some of the more successful fits using only Born amplitudes and using Born amplitudes plus various resonance models. Symbols are defined in the text. In general, Eq. (7a) has been used for combining resonant and nonresonant amplitudes. Subscripts b and c on the solution number denote the use of Eqs. (7b) and (7c).

Resonant amplitude	Solution number n	$\frac{g_\Lambda}{(4\pi)^{1/2}}$	$\frac{G_\Sigma}{(4\pi)^{1/2}}$	$\frac{G_V}{4\pi}$	$\frac{G_T}{4\pi}$	$\Gamma^0_{M_{l\pm}}$ (MeV)	$\Gamma^0_{E_{l\pm}}$ (MeV)	Γ (MeV)	W_0 (MeV)	χ_σ^2	χ_P^2	χ^2/N
None	1	2.57	1.52	0.105	0.064					154		3.67
	2	2.49	1.16	0.226	−0.062					155		3.69
$P_{1/2}(M_{1-})$	3	2.33	0.90	0.144	0.024	0.360		107	1673	86	15.0	2.16
	4	2.59	1.58	0.129	0.048	0.389		108	1676	93	14.3	2.27
	5_a	2.33	0.68	0.134	0.002	0.426		120	1672	88	14.8	2.19
	5_b	2.32	0.68	0.134	0.001	0.422		120	1671	92	14.5	2.27
	5_c	2.33	0.68	0.134	0.002	0.426		120	1672	93	12.1	2.23
$P_{3/2}(M_{1+})$	6	1.60	−0.61	0.001	0.134	0.464		272	1631	133	7.9	3.00
	7	1.39	−0.82	−0.009	0.171	0.407		144	1694	156	10.9	3.56
	8	1.19	−1.62	−0.028	0.137	0.404		138	1697	152	13.1	3.51
$P_{3/2}(M_{1+}+E_{1+})$	9	1.77	−1.60	−0.108	0.045	0.787	−0.260	169	1697	131	15.2	3.15
$D_{3/2}(M_{2-})$	10	1.91	−1.59	0.023	−0.134	0.219		82	1666	119	14.2	2.83
	11	2.06	−1.91	0.035	−0.230	0.216		96	1674	144	14.5	3.38
$D_{3/2}(E_{2-})$	12	2.37	−0.40	0.105	−0.147		0.324	111	1692	205	6.7	4.51
	13	2.29	−0.59	0.177	−0.197		0.431	119	1694	206	6.3	4.51
$D_{3/2}(M_{2-}+E_{2-})$	14_a	2.04	0.06	0.089	−0.015	0.262	0.198	96	1651	67	6.3	1.59
	14_b	2.11	0.04	0.086	−0.011	0.246	0.213	112	1650	85	6.3	1.98
	14_c	2.08	0.04	0.085	−0.013	0.290	0.251	132	1648	81	5.0	1.87
	15	1.97	−1.89	0.087	−0.237	0.266	0.217	99	1666	99	5.9	2.28
	16	2.42	0.57	0.163	−0.096	0.252	0.406	101	1680	114	4.2	2.57
$F_{5/2}(E_{3-})$	17	2.33	−0.20	0.061	−0.074		0.157	100	1688	161	36.7	4.22
$F_{5/2}(M_{3-}+E_{3-})$	18	2.38	0.63	0.118	−0.001	−0.074	0.097	101	1682	166	17.4	3.98
	19_a	2.28	0.07	0.165	−0.092	−0.152	−0.078	98	1681	152	18.4	3.70
	19_b	2.29	0.06	0.165	−0.092	−0.138	−0.039	100	1681	160	17.3	3.86
	19_c	2.29	0.06	0.165	−0.092	−0.141	−0.047	100	1682	158	17.5	3.80
	20	2.09	−1.70	0.132	−0.254	−0.214	−0.125	101	1684	184	18.0	4.40

resonance fits are made using Eq. (7a) except those with subscripts b and c on the solution number n. For these cases the parameters of the a solution are used as the initial parameters in the optimization program, and Eqs. (7b) and (7c) are used for the resonant state form. In most cases, the results are insensitive to which of the various forms of Eq. (7) is used. However, in the case of solutions 6, 7, and 8, no good fits were found when Eq. (7b) was used; here the Born M_{1+} amplitude is large and whether it is included or not becomes important.

Resonant states for which no satisfactory fits were obtained are not included in Table I. An S-wave resonance [E_{0+} using Eq. (7b)] tends to give fits which are similar to the Born solutions. The optimum size of the resonant amplitude is so small that very little polarization results. An E_{1+} ($P_{3/2}$) resonance gives very bad χ^2 fits, probably because of the large size of the Born amplitude which is subtracted. The $D_{5/2}$ resonance assumptions (E_{2+}, M_{2+}, and $E_{2+}+M_{2+}$)[32] all give $\chi^2/N>5$. Finally, a pure M_{3-} ($F_{5/2}$) resonance also gives large χ^2 fits.

The value of χ^2/N is never as good as the "expected" value of 1. Actually it would be rather remarkable if the simple model used could give values as low as 1, and it is difficult to estimate the effect of systematic experimental errors which are not included in the statistical errors given in Table IV. Fits for which $\chi^2/N\approx 3$ are not uncommon in treatments similar to this.[19]

Solutions 1 and 2 show that the Born amplitudes alone give quite good fits to the cross-section data. Only M_{1-} ($P_{1/2}$) and $M_{2-}+E_{2-}$ ($D_{3/2}$) resonances give reasonable polarization fits and also improve χ_σ^2 appreciably over the values obtained with Born amplitudes alone. Though the optimum resonance energies appear to be low the maximum resonance contributions to the cross section occur near 1.7 GeV. The $F_{5/2}$ resonance assumptions do not give particularly good fits to the cross sections and yield values which are too small for the polarization.

Figure 2 shows the comparison of the Born solution 2 with some of the experimental cross-section angular distributions. Figure 3 compares solutions 3, 14a, and 19a ($P_{1/2}$, $D_{3/2}$, and $F_{5/2}$ resonances) with the same experimental data. The 1.4-GeV data have not been used in the χ^2 fits so the calculated curves just show the extrapolation of the various models to this energy. If the 1.4-GeV data were included, the χ^2 of the lower energy data would be increased. Below 1.0 GeV, the $D_{3/2}$ solution fits the data of Ref. 9 and 25 best, though all solutions tend to be too high here.

Figure 4 shows the fit of solutons 3, 14a, and 19a to the polarization data. Here the differences in the calculated curves are larger but the experimental statistics are poor. The datum at 61° has not been used in the fits and none of the three solutions plotted agrees very well with it. The inclusion of this point in the χ^2 optimization would have little effect, and much more polarization data as a function of angle would be necessary to determine the characteristic shape of the polarization angular distribution.[39]

The larger partial-wave amplitudes which are given by solutions 3 and 14a are shown in Figs. 5 and 6. The nonresonant amplitudes are typical of those which any of the solutions yield. S and $P_{3/2}$ amplitudes are most important with nonresonant waves of higher angular momentum becoming important only at the larger energies. In general, the $P_{1/2}$ amplitude seems to be considerably smaller than the $P_{3/2}$ amplitudes. The effect on the differential cross section of partial waves higher than $F_{5/2}$ is shown in Fig. 2 for Born solution 2. The deviation from the exact Born cross section is small if the partial-wave expansion is summed through $F_{5/2}$.

It is clear from Table I that the results are not sensitive to many of the parameters or that the parameters are interrelated so that a change in one can be compensated for by changes in the others. The value of g_A has the most influence on the fits and only it remains relatively constant. The number of trials used in the χ^2 optimization is not large enough to find unambiguously the regions of each parameter for which good fits can be obtained. However, for the small number of successful fits which are found, a tabulation of the maximum and minimum values of each parameter can be made and is given in Table II. In comparing the various parameters with the results of other determinations, it probably is better to use the values of Table

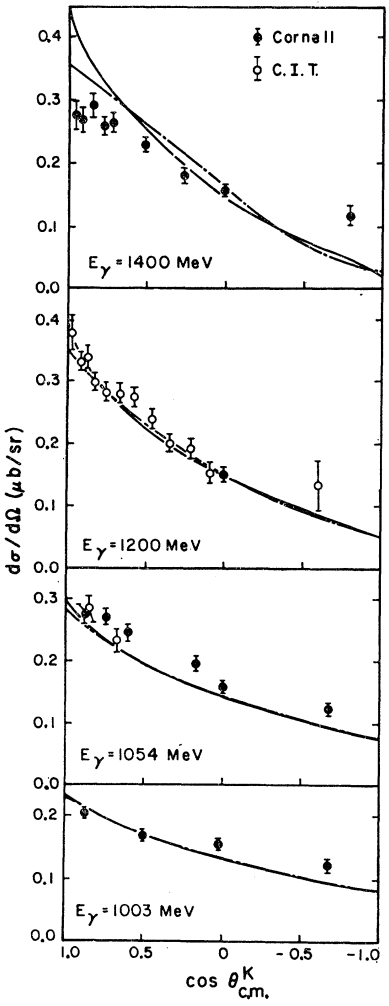

FIG. 2. Comparison of the cross-section data with a solution which contains only nonresonant Born terms. Solid line is exact calculation using the parameters of solution (2) (Table I). Dashed line shows the approximate calculation for the same solution where partial waves through $F_{5/2}$ only are used. The 1400-MeV data are not used in the χ^2 optimization.

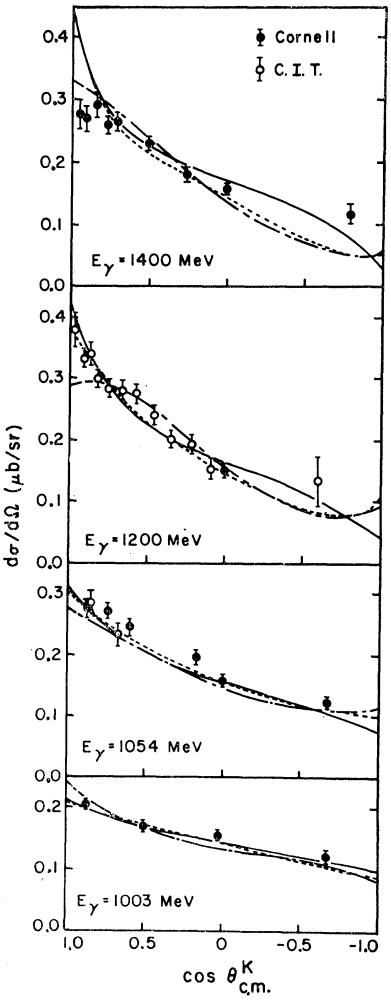

FIG. 3. Comparison of the cross-section data with fits which have $P_{1/2}$ (solid line), $D_{3/2}$ (dashed line), and $F_{5/2}$ (dot-dashed line) resonant amplitudes. Table I gives the parameters used in these fits [solutions (3), (14a), (19a)]. The 1400-MeV data are not used in the χ^2 optimization.

[39] J. Dufour's $F_{5/2}$ fits (Ref. 2) give better agreement with the 61° polarization point than solution (19a). This is because Γ^0_{E3-} has the opposite sign from Γ^0_{M3-} in (19a). Solution (18) is similar to his solutions in this respect and fits the 61° point better than solution (19a).

II rather than the best solutions given in Table I which do not indicate the sensitivity of the parameters.

V. DISCUSSION AND COMPARISON WITH PREVIOUS CALCULATIONS AND THE PREDICTIONS OF $SU(3)$

The solutions given in Table I show that $P_{1/2}$, $D_{3/2}$, $F_{5/2}$, and possibly $P_{3/2}$ resonant amplitudes all give reasonable fits to the data. In most of the solutions the resonant amplitudes are found to contribute less than 25% to the integral cross section. In other words, the data are singularly insensitive to what resonant state is chosen to emend the Born amplitudes. The $P_{1/2}$ and

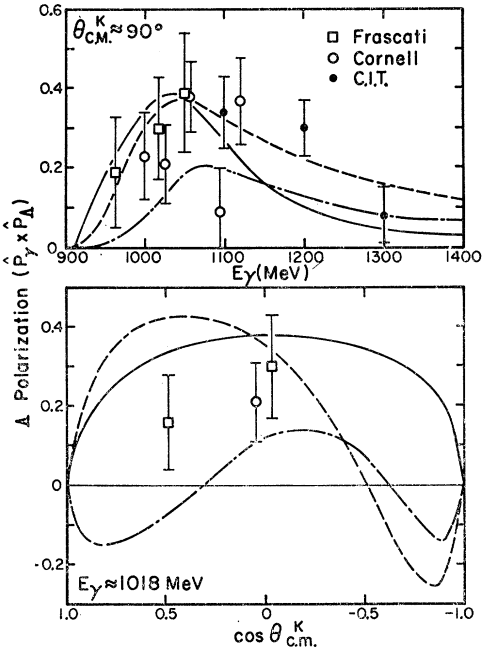

FIG. 4. Comparison of the experimental polarization with solutions (3) (solid line, $P_{1/2}$), (14a) (dashed line, $D_{3/2}$), and (19a) (dot-dashed line, $F_{5/2}$). The 61° point is not used in the χ^2 optimization.

$D_{3/2}$ resonances are favored but not sufficiently to rule out the other possibilities. Very likely, mixtures of different resonant state amplitudes (e.g., $P_{1/2}$ and $F_{5/2}$ resonances both near 1.7 GeV) would give good fits. Also, other means of generating an imaginary amplitude probably could be made to fit the data (e.g., a resonance below threshold so that just the tail of the resonant amplitude is present in our energy region). The apparent unimportance of resonant amplitudes indicates that a more thorough evaluation of Born amplitudes including the second πN resonance and Y^* exchange might lead to a relatively accurate coupling constant determination.

The results found here are to be compared with the previous results of other authors, in which only an $F_{5/2}$ resonance has succeeded in explaining the observed polarization. A summary of the previous papers can

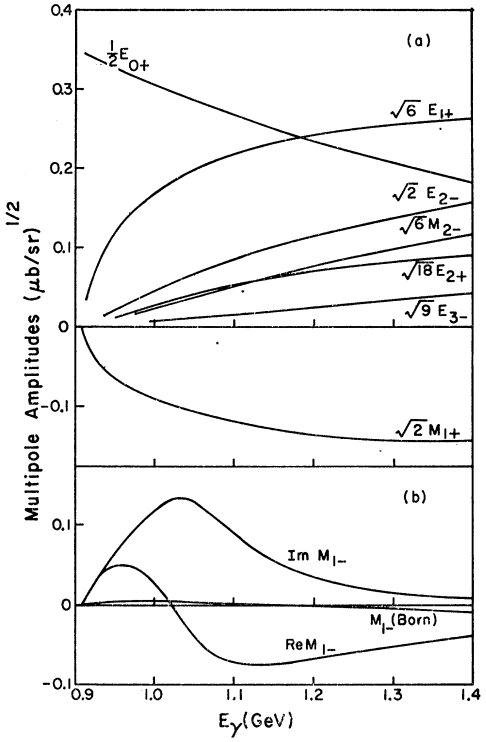

FIG. 5. The larger multipole amplitudes as a function of photon energy for solution (3) with a M_{1-} resonant state. The normalization of the various amplitudes is $[\frac{1}{4}(2J+1)j_\gamma(j_\gamma+1)]^{1/2}$ so that the contribution to the total cross section is just $4\pi q/k$ times the square of the ordinate value independent of j_γ and J (see Appendix I). E_{0+} has in addition an arbitrary scale factor of $\frac{1}{2}$ and consequently contributes 4 times the square of the ordinate value. (a) The nonresonant background amplitudes; (b) the real and imaginary parts of the resonant amplitude along with the M_{1-} Born amplitude which has been subtracted out.

be found in Ref. 15 so we will mention only the obvious differences between this work and previous work. On the whole, more terms are included in this calculation; with the exception of Dufour's work no effort has been made in previous calculations to optimize χ^2. Fayyazuddin[5] uses only Born amplitudes derived from those couplings which we associate with the constants g_Λ, G_Σ, and G_V. Beauchamp and Holladay,[3] and Kuo[4] use terms derived from couplings associated with g_Λ, G_V, and G_T; the Λ and Σ exchange diagrams are ignored (i.e., $\kappa_\Lambda g_\Lambda + \kappa_T g_{2KN} = 0$). Both papers consider a $P_{1/2}$ resonance but find the direction of the polarization opposite to the observed direction (the sign of their $\Gamma^0{}_{M_{l\pm}}$ is opposite to that found here). Kuo also tries E_{1+} and M_{1+} resonant amplitudes, but here again is unable to fit the polarization.[40] Hatsukade and Schnitzer[1] use a model in which Mandelstam dispersion relations are employed to generate amplitudes associated with the K^* and with the second and third πN resonances. Pole terms are associated with the constants

[40] There also seem to be computational errors in Kuo's paper.

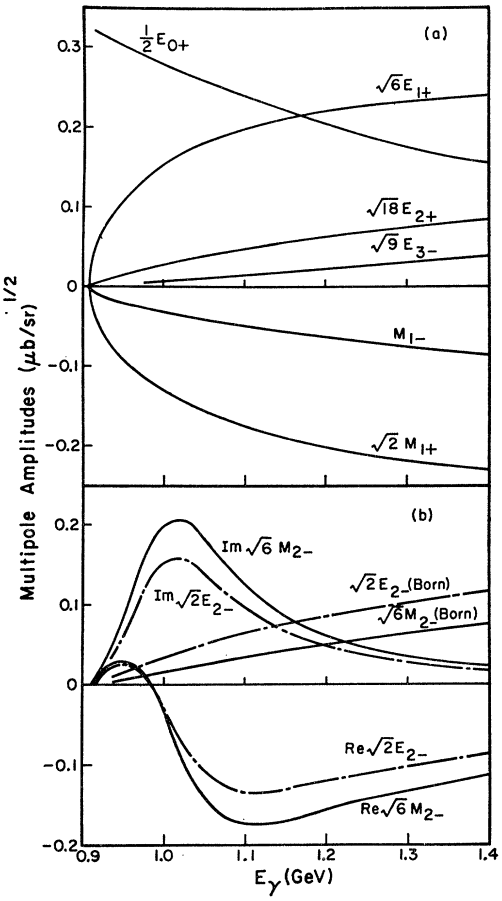

FIG. 6. The large multipole amplitudes for solution (14a) with M_{2-} and E_{2-} resonant amplitudes. Normalization is similar to that in Fig. 5.

g_Λ, g_Σ, κ_Λ, and κ_T. These authors are able to get the correct sign for the polarization but it tends to be too small at higher energies. Their coupling constant ($g_\Lambda^2/4\pi \approx 1.4$) is rather small compared with the value obtained by others. Hatsukade, Pandit, and Zimerman[1] do not try to fit the data exactly but only wish to show that a large g_Λ [the $SU(3)$ value] can be used in conjunction with the $P_{1/2}$ ($\approx$1400 MeV) resonance of Roper[19] to obtain cross sections which are of the same magnitude as the observed values. Dufour[2] uses the Born couplings associated with g_Λ, G_Σ, and G_V along with an $F_{5/2}$ resonance. His fits are in good agreement with the low-energy data and, when modified so as to fit the higher energy data, yield χ^2's which are approximately the same as found here for an $F_{5/2}$ resonance.

From our fits, it seems unlikely that Born and $F_{5/2}$ resonance terms alone can explain the data. The calculated cross section using this resonance has a tendency to turn down at forward angles for energies above the resonance energy (see Fig. 3). The 1200-MeV data have exactly the opposite behavior; more measurements at very forward angles should remove any doubt as to the importance of an $F_{5/2}$ resonance.

If any of the various fits found here have physical meaning, one should be able to fit the (πp, $K\Lambda$) data with an analogous model. This model should yield values of the coupling constants $g_{K\Lambda N}$, $g_{K\Sigma N}$, $g^V{}_{K^*\Lambda N}$, and $g^T{}_{K^*\Lambda N}$ which are similar to our values, and it should employ the same resonant state. Of course the values of some of the coupling constants are not well restricted because of the various unknown coupling constants which multiply them. In an analysis of the (πp, $K\Lambda$) reaction, Hoff[7] does find an indication of a $P_{1/2}$ resonance at 1700 MeV with a width of 64 MeV. However, only K^* vector coupling exchange is used to generate the nonresonant background. The estimated strength of the $g^V{}_{K^*\Lambda N}$ coupling constant from her analysis is $g^V{}_{K^*\Lambda N}{}^2/4\pi \approx 0.17$.

If the resonance is indeed found to be $P_{1/2}$, the circumstance that it shows up strongly in the (πp, $K\Lambda$) system whereas it is hardly discernible in the (γp $K\Lambda$) reaction might be explained by the small $P_{1/2}$ Born

TABLE II. The ranges of parameter values for which reasonable fits to the data are found for Born terms and for various resonance models.

Resonant amplitude		$\frac{g_\Lambda}{(4\pi)^{1/2}}$	$\frac{G_\Sigma}{(4\pi)^{1/2}}$	$\frac{G_V}{4\pi}$	$\frac{G_T}{4\pi}$	$\Gamma^0{}_{M_{l\pm}}$ (MeV)	$\Gamma^0{}_{E_{l\pm}}$ (MeV)	Γ (MeV)	W_0 (MeV)	χ^2/N
None	min	2.31	−0.35	0.047	−0.118					3.67
	max	2.61	1.61	0.226	0.066					5.00
$P_{1/2}(M_{1-})$	min	2.31	0.68	0.126	0.001	0.316		107	1668	2.16
	max	2.61	1.69	0.146	0.079	0.439		120	1676	2.58
$P_{3/2}(M_{1+})$	min	1.10	−1.98	−0.039	0.122	0.188		135	1631	3.00
	max	1.60	−0.59	0.001	0.171	0.990		271	1698	3.56
$D_{3/2}(M_{2-})$	min	1.89	−1.91	0.020	−0.230	0.188		82	1666	2.83
	max	2.07	−1.59	0.035	−0.134	0.252		96	1674	3.44
$D_{3/2}(M_{2-}+E_{2-})$	min	1.93	−1.92	0.085	−0.239	0.089	0.140	96	1648	1.59
	max	2.43	0.57	0.208	0.000	0.585	0.623	135	1697	2.72
$F_{5/2}(M_{3-}+E_{3-})$	min	2.07	−1.72	0.116	−0.255	−0.214	−0.126	98	1680	3.70
	max	2.38	0.65	0.167	0.000	−0.062	0.141	103	1684	4.40

amplitude found here.[41] If the photoproduction resonant amplitude is generated by multiplying the Born amplitude by a term proportional to $\sin\delta e^{i\delta}$, as described in Sec. II above, then a small resonant amplitude would result.

The values of the coupling constants given in Tables I and II in principle can be compared with values predicted by $SU(3)$. However, the predicted values are often arrived at by tenuous arguments which make use of only approximately known constants; moreover, the experimental values found here suffer from all the uncertainties of our model. Thus one can hope for only rough agreement.

The coupling constants $g_{K\Lambda N}$, $g_{K\Sigma N}$, $g^V{}_{K^*\Lambda N}$, and $g^T{}_{K^*\Lambda N}$ are related to the coupling constants $g_{\pi NN}$, $g^V{}_{\rho NN}$, and $g^T{}_{\rho NN}$ by[42,43]

$$\begin{aligned} g_{K\Lambda N}&=-(1/\sqrt{3})(3-2\alpha)g_{\pi NN}\,,\\ g_{K\Sigma N}&=(2\alpha-1)g_{\pi NN}\,,\\ g^V{}_{K^*\Lambda N}&=-(1/\sqrt{3})(3-2\alpha_E)g^V{}_{\rho NN}\,,\\ g^T{}_{K^*\Lambda N}&=-(1/\sqrt{3})(3-2\alpha_M)g^T{}_{\rho NN}\,, \end{aligned} \tag{10}$$

where α, α_E, and α_M are the F to D mixing parameters for PBB, VBB^V, and VBB^T couplings $[D/F=\alpha/(1-\alpha)]$. The values of α, α_E, and α_M are not known accurately but standard choices are[42–45]

$$\begin{aligned} &0.60\leq\alpha\leq0.75\,,\\ &\alpha_E\approx0\,,\\ &\alpha_M\approx\tfrac{3}{4}\,. \end{aligned}$$

The πNN coupling constant is well known

$$(g_{\pi NN}{}^2/4\pi\approx15)$$

but the ρNN^V and ρNN^T coupling constants can only be estimated from models of πp and pp scattering. The coupling constants are given by[45–47]

$$0.55\leq g^V{}_{\rho NN}{}^2/4\pi\leq1.27\,,$$

and

$$g^T{}_{\rho NN}{}^2/4\pi\approx11.4\,.$$

The ratio $(g^T{}_{\rho NN}/g^V{}_{\rho NN})$ is given in terms of the Pauli and Dirac magnetic moments if one associates the isovector form factors of electron-nucleon scattering with the exchange of a ρ meson. The ratio is

$$g^T{}_{\rho NN}/g^V{}_{\rho NN}=\mu_p-\mu_n=3.7\,,$$

where μ_p and μ_n are the anomalous magnetic moments. This ratio is consistent with the values of the coupling constants given above. The Λ, Σ transition magnetic moment predicted from $SU(3)$ is $\mu_T=-(\sqrt{3}/2)\mu_n$ or $\kappa_T=2.0$.[48]

The decay rate of $K^{*+}\to K^++\gamma$ can be estimated from the partial decay width of the ω into $\pi^0+\gamma$ given by $\Gamma_{\omega\to\pi^0\gamma}=1.2$ MeV.[49] In the limit of equal masses the matrix element M of $\omega_8\to\pi^0+\gamma$ is related to that of $K^{*+}\to K^++\gamma$ by[50]

$$M(K^{*+}\to K^+\gamma)/M(\omega_8\to\pi^0\gamma)=1/\sqrt{3}\,.$$

If one assumes a p^3 phase space (where p is the momentum of the decay particles in the rest system of the K^* or ω), an ω-ϕ mixing angle, θ, given by[51] $\sin^2\theta=0.4$, and a negligible decay width of the ϕ into $\pi^0+\gamma(\Gamma_{\phi\to\pi^0\gamma}\approx0)$, one finds[52]

$$\Gamma_{K^{*+}\to K^+\gamma}=\tfrac{1}{3}\sin^2\theta(p_K/p_\pi)^3\Gamma_{\omega\to\pi^0\gamma}\,,$$

or

$$\Gamma_{K^{*+}\to K^+\gamma}\approx0.086\text{ MeV}\,,$$

and

$$g_{K^{*+}K^+\gamma}{}^2/4\pi=1/115\,.$$

The dimensionless coupling constant $g_{K^{*+}K^+\gamma}$ is associated with an arbitrary normalizing mass which we have chosen to be 1 GeV. (The definition of $g_{K^{*+}K^+\gamma}$ can be found in Appendix I.)

The expected $SU(3)$ values of g_Λ, G_Σ, G_V, and G_T can now be written

$$\begin{aligned} g_\Lambda/(4\pi)^{1/2}&=(1/\sqrt{3})(3-2\alpha)(g_{\pi NN}{}^2/4\pi)^{1/2}\,,\\ G_\Sigma/(4\pi)^{1/2}&=(1-2\alpha)\kappa_T(g_{\pi NN}{}^2/4\pi)^{1/2}\,,\\ |G_V/4\pi|&=(1/\sqrt{3})(3-2\alpha_E)(g^V{}_{\rho NN}{}^2g_{K^*K\gamma}{}^2)^{1/2}/4\pi\,,\\ |G_T/4\pi|&=(1/\sqrt{3})(3-2\alpha_M(g^T{}_{\rho NN}{}^2g_{K^*K\gamma}{}^2)^{1/2}/4\pi\,, \end{aligned} \tag{11}$$

and

$$G_T/G_V=(\mu_p-\mu_n)(3-2\alpha_M)/(3-2\alpha_E)\,.$$

[41] The $P_{1/2}$ Born amplitude may be small only because we have disregarded the Y^* exchange diagrams. See P. Carruthers, Phys. Rev. **133**, B497 (1964).

[42] M. Gell-Mann and Y. Ne'eman, *The Eightfold Way* (W. A. Benjamin, Inc., New York, 1964).

[43] P. Carruthers, *Introduction to Unitary Symmetry* (Interscience Publishers, Inc., New York, 1966); P. Carruthers, *Lectures in Theoretical Physics* (University of Colorado Press, Boulder, Colorado, 1965), Vol. VIIb, p. 82. Both these references and Ref. 42 are general sources for the $SU(3)$ results used here.

[44] B. Sakita and W. C. Wali, Phys. Rev. **139**, B1355 (1965); A. W. Martin and K. C. Wali, Nuovo Cimento **31**, 1324 (1964).

[45] J. J. Sakurai, in *Proceedings of the International Summer School "Enrico Fermi", Course XXVI* (Academic Press Inc., New York, 1963); J. J. Sakurai, Nuovo Cimento **34**, 1582 (1964).

[46] J. D. Jackson and H. Pilkuhn, Nuovo Cimento **33**, 906 (1964).

[47] J. W. Durso and P. Signell, Phys. Rev. **135**, B1057 (1964). Probably the estimate of $g^V{}_{\rho NN}\approx0.5$ from πp scattering (Ref. 45) is the best; the p-p scattering analyses are not consistent among themselves. For an estimate from electromagnetic form factors see J. S. Ball and D. Y. Wong, Phys. Rev. **133**, B179 (1964).

[48] S. Coleman and S. L. Glashow, Phys. Rev. Letters **6**, 423 (1961), or Ref. 42; N. Cabibbo and R. Gatto, Nuovo Cimento **21**, 872 (1961), or Ref. 42.

[49] A. H. Rosenfeld, A. Barbaro-Galtieri, W. H. Barkas, P. L. Bastien, J. Kirz, and M. Roos, Rev. Mod. Phys. **37**, 633 (1965).

[50] S. Okubo, Phys. Letters **4**, 14 (1963), or Ref. 42.

[51] S. L. Glashow, Phys. Rev. Letters **11**, 48 (1963), or Ref. 42; D. F. Dashen and D. H. Sharp, Phys. Rev. **133**, B1585 (1964), or Ref. 42.

[52] For nonet coupling model, see S. L. Glashow and R. H. Socolow, Phys. Rev. Letters **15**, 329 (1965).

Here the signs of g_Λ and G_Σ have been changed to correspond to the convention of this paper ($g_\Lambda>0$). As α_M varies from $\frac{3}{4}$ to 1.0 and as the other parameters in Eqs. (11) take on their above indicated values (or range in values), Eqs. (11) have the following numerical limits:

$$\begin{aligned} 3.3 \leq & g_\Lambda/(4\pi)^{1/2} \leq 4.0, \\ -4.0 \leq & G_\Lambda/(4\pi)^{1/2} \leq -1.5, \\ 0.12 \leq & |G_V/4\pi| \leq 0.18, \\ 0.18 \leq & |G^T/4\pi| \leq 0.27, \end{aligned}$$

and

$$0.54 \leq G_V/G_T \leq 0.81.$$

The above is to be compared with the calculated values of Tables I and II. These calculated values of the parameters fall approximately within ranges given by

$$\begin{aligned} 1.1 \leq & g_\Lambda/(4\pi)^{1/2} \leq 2.6, \\ -2.0 \leq & G_\Sigma/(4\pi)^{1/2} \leq 1.7, \\ -0.04 \leq & G_V/4\pi \leq 0.23, \\ -0.26 \leq & G_T/4\pi \leq 0.17. \end{aligned}$$

The ratio G_V/G_T varies widely; typically G_T is too small and of the wrong sign compared with G_V to give the predicted ratio.

All things considered, the agreement between the values expected from $SU(3)$ and the values given in Tables I and II is reasonable though rather inconclusive.[53] It has long been noted that experimentally g_Λ appears to be smaller than the $SU(3)$ value; actually the two values agree if $\alpha\approx 1.0$ is used.[2] Arbitrarily choosing α so that the experimental and predicted coupling constants agree exactly is possibly not very realistic in the light of the many explanations for the discrepancy; however, it is interesting that Dufour also gets a value of α close to 1 from the $g_{K\Sigma N}$ coupling constant in his analysis of $\gamma+p\rightarrow K+\Sigma^0$. The experimental value of G_Σ compared with the $SU(3)$ value is too small and in some of the fits it has a sign opposite to that which is expected. Dufour[2] has pointed out that the experimentally derived value of G_Σ may be inaccurate owing to contamination from the effects of the Y^* exchange.[54] The expected and calculated values of G_V are in remarkable agreement. If the estimate of $\Gamma_{K^{*+}\rightarrow K^+\gamma}$ can be believed, then the calculated value of $g^V{}_{K^*\Lambda N}$ ($g^V{}_{K^*\Lambda N}{}^2/4\pi\approx\frac{3}{4}$ to 4) agrees well with the value predicted by $SU(3)$ ($1.5\leq g^V{}_{K^*\Lambda N}{}^2/4\pi\leq 3.8$). Hoff,[7] in her analysis of (πp, $K\Lambda$), finds $g^V{}_{K^*\Lambda N}{}^2$ about $\frac{1}{10}$ the expected value, but this may be because the direct nucleon and Σ exchange diagrams are not considered. The experimental value of G_T does not compare at all well with the expected value; it is consistently too small. The fact that G_T is too small whereas G_V agrees well with the $SU(3)$ value may indicate that α_M is larger than previously estimated. A value of $\alpha_M\approx 1.5$ would be consistent with the small value of G_T, though it is in marked disagreement with present theory.

If one assumes that the πN resonances, $D_{3/2}$ (1518) and $F_{5/2}$ (1688), are members of octets, then their contributions to the (γp, $K\Lambda$) and (πp, $K\Lambda$) reactions can be estimated from the elastic πp and the $\gamma p\rightarrow\pi N$ cross-section data.[30,43,55] $SU(3)$ predicts the ratio of the reduced widths γ of the πN and $K\Lambda$ systems. This ratio for an octet resonant state decaying into octets is

$$\gamma_{K\Lambda}/\gamma_{\pi N}\approx 2/7 \quad \text{for} \quad \alpha=0.7.$$

Unfortunately, in general the estimated contributions to the cross sections depend more upon the form of the centrifugal barrier penetration factor which is used than on the predicted γ. For example, the $F_{5/2}$ resonance contribution to the $K\Lambda$ system will be considerably different if we use Glashow and Rosenfeld's form of $v_l(qR)$[30] instead of the nuclear physics form of Blatt and Weisskopf (see Ref. 27 and Appendix I). Glashow and Rosenfeld use $v_l(qR)$ defined by

$$v_l(qR)=\{(qR)^2/[1+(qR)^2]\}^l. \tag{12}$$

The amount of resonance contribution also depends on the value of the interaction radius R which is chosen. Glashow and Rosenfeld use an R given by $1/R=350$ MeV, and Carruthers[55] suggests $1/R=1$ GeV, whereas we have used $1/R=200$ MeV.

An estimate of the contributions of the second and third resonances to the (γp, $K\Lambda$) partial-wave amplitudes may now be made, using the known contributions of these resonances to the (γp, πN) integral cross sections.[56] Calculations are performed for three choices of $v_l(qR)$: (a) $v_l(qR)$ of Appendix I, $1/R=200$ MeV; (b) $v_l(qR)$ of Eq. (12), $1/R=350$ MeV; (c) $v_l(qR)$ of Eq. (12), $1/R=1.0$ GeV. [Numerical values calculated below will be denoted (a), (b), or (c) to indicate which choice has been used.] Using Eqs. (3), (6), and (A11) the contribution to the integral cross section at W_0 from a resonant amplitude is

$$\sigma(M_{l\pm})+\sigma(E_{l\pm})=\frac{4\pi}{(k^0)^2}\frac{J+\frac{1}{2}}{2}\frac{(\Gamma^0{}_{M_{l\pm}})^2+(\Gamma^0{}_{E_{l\pm}})^2}{\Gamma^2}, \tag{13}$$

where

$$(\Gamma^0{}_{M_{l\pm}})^2=\Gamma^0{}_M\Gamma^0{}_{l\pm}=\Gamma^0{}_M q^0 R v_l{}^0(qR)\gamma$$

and similarly for $\Gamma^0{}_{E_{l\pm}}{}^2$. Thus the ratio of $(\Gamma^0{}_{M_{l+}})^2$ for the $K\Lambda$ and πp systems evaluated for the $F_{5/2}$ resonance

[53] Of course the cross sections computed using the $SU(3)$ coupling constants are in very poor agreement with the experimentally observed cross sections.

[54] J. Dufour finds $g_{K\Sigma N}{}^2/4\pi\approx 12$ in his (γp,$K\Sigma$) analysis. This result implies that either μ_T is very small or G_Σ is inaccurate.

[55] P. Carruthers, Phys. Rev. Letters **12**, 259 (1964).

[56] R. L. Walker, in Proceedings of the Conference on Photon Interactions in the BeV Energy Range, Massachusetts Institute of Technology, Cambridge, Massachusetts, 1963 (unpublished).

is

$$\frac{\Gamma^0{}_{M_{3-}}(K\Lambda)^2}{\Gamma^0{}_{M_{3-}}(\pi N)^2}=\frac{q_K{}^0v^0{}_l(q_KR)\gamma_{K\Lambda}}{q_\pi{}^0v_l{}^0(q_\pi R)\gamma_{\pi N}}\approx \begin{cases} 3\times10^{-3} & \text{(a)} \\ 10\times10^{-3} & \text{(b)} \\ 1\times10^{-3} & \text{(c)}. \end{cases} \quad (14)$$

The expression for $(\Gamma^0{}_{E_{3-}})^2$ is identical. The third resonance contributes about 30 μb to the $T=\frac{1}{2}$ $(\gamma p, \pi N)$ cross section at W_0, so by Eqs. (13) and (14) the $K\Lambda$ partial width is expected to be

$$[\Gamma^0{}_{M_{3-}}(K\Lambda)^2+\Gamma^0{}_{E_{3-}}(K\Lambda)^2]^{1/2}\approx \begin{cases} 0.20 \text{ MeV} & \text{(a)} \\ 0.36 \text{ MeV} & \text{(b)} \\ 0.12 \text{ MeV} & \text{(c)}. \end{cases}$$

The partial widths obtained using barrier factors (a) and (c) are quite consistent with the widths found for the $F_{5/2}$ resonance in the phenomenological fits. From Table I the average value of $[(\Gamma^0{}_{M_{3-}})^2+(\Gamma^0{}_{E_{3-}})^2]^{1/2}$ is approximtely 0.16 MeV.

If we apply the arguments used above to the $(\pi p, K\Lambda)$ reaction, then the maximum contribution of the third resonance to the integral cross section is: 140 μb (a), 350 μb (b), and 60 μb (c) [or the ratio of the partial widths to the total width is $\Gamma_i\Gamma_f/\Gamma^2\approx1/530$ (a), 1/160 (b), 1/1400 (c)]. The observed enhancement in the $(\pi p, K\Lambda)$ reaction is approximately 500 μb.

It seems likely that a small contribution of the $F_{5/2}$ third resonance can be present in both the $(\gamma p, K\Lambda)$ and $(\pi p, K\Lambda)$ reactions. Uto *et al.*[8] and Anderson *et al.*[57] both find indication of F-wave amplitudes from their $(\pi p, K\Lambda)$ polarization data in an incident momentum range of 1025 to 1050 MeV/c. However, an $F_{5/2}$ resonance does not seem to be the dominant cause of either the polarization in the $(\gamma p, K\Lambda)$ reaction or of the enhancement in the $(\pi p, K\Lambda)$ cross section.

The $D_{3/2}$ second resonance (1518) is predominantly E_{2-} and contributes about 60 μb to the $(\gamma p, \pi N)$ system at resonance. The predicted $SU(3)$ contribution of the resonance to the $(\gamma p, K\Lambda)$ system can be estimated using Eq. (2) with $\Gamma\approx120$ MeV and gives $|\sqrt{2}\,\mathrm{Re}E_{2-}(N^{**})|$ in the range of 0.14 to 0.20 $(\mu\text{b/sr})^{1/2}$ for E_γ in the range of 1050 to 1200 MeV and for all three forms of $v_l(qR)$. (The imaginary part of the amplitude is about 25% of the real part.) It can be seen from Figs. 5 and 6 that the above estimate is about twice the size of the E_{2-} Born amplitude in the same energy region, so possibly it has been unwise to disregard the second resonance in our model.

VI. CONCLUSIONS

Good fits to the $(\gamma p, K\Lambda)$ experimental data are found using a model which contains perturbation amplitudes and a resonant amplitude in one l, J state. The couplings which are used for the perturbation amplitudes include both the standard Born couplings and vector meson exchange. The coupling constants which are found from the fits are generally smaller than the expected $SU(3)$ values; those associated with the K^* tensor exchange and Σ exchange diagrams are considerably smaller than expected. The largest partial-wave amplitudes from the perturbation terms are found to be E_{0+}, E_{1+}, and M_{1+}. The fits are found to be relatively insensitive to the choice of resonant state and in most cases the resonance contributes a maximum of 10–30% to the integral cross section. The best fits are obtained for $P_{1/2}$ and $D_{3/2}$ resonant states. It is felt that the results of this paper have little validity unless an analogous model with a similar resonant state and similar coupling constants can be found in an analysis of the $(\pi p, K\Lambda)$ reaction.

An $F_{5/2}$ resonance with a small partial width is consistent with the data though it seems likely that it is not the main cause of the polarization. The phenomenological partial width found for this resonant state is in agreement with a rough estimate of the strength of the πN third resonance in this channel. A similar estimate of the importance of the πN second resonance indicates that it possibly should not have been ignored in the analysis.

An estimate of the importance of the Y^* exchange diagrams should be made. The values of the other coupling constants found here may deviate from their actual values because we have not included the Y^* terms; also the nonresonant partial-wave amplitudes may be unreliable for the same reason. In particular, the $P_{1/2}$ Born amplitude M_{1-} is small in our solutions, but this may no longer be the case if Y^* exchange is considered.[58]

A physically more interesting and reasonable model than the one used here might include Y^* exchange amplitudes in addition to the amplitudes associated with the diagrams of Fig. 1. Such a model might also include terms associated with the second and third πN resonances, along with a $P_{1/2}$ resonance as the main cause of the polarization. However, as a result of its very complexity, this more intricate model may not add significantly to our understanding.

Perhaps the most significant result of this analysis is that it points out the dangers involved in using a phenomenological model to fit the data and considering only the most popular hypothesis without attempting to explore the sensitivity of the fits when that hypothesis is changed or modified. Intuitive feelings are supported or strongly emphasized by this analysis in the following respects. First, the experimental results do not have enough characteristic features to lend themselves to unambiguous interpretation and they are not dominated by one particular outstanding phenomenon. Secondly, the theory is *ad hoc* in nature and the analysis of this

[57] J. A. Anderson *et al.*, in *Proceedings of the 1962 International Conference on High Energy Physics*, edited by J. Prentki (CERN, Geneva, 1962).

[58] P. Carruthers, Phys. Rev. **133**, B497 (1964); also Ref. 43.

reaction alone is not sufficiently restrictive to prove generally the usefulness and consistency of such theories. Finally, if more $K\Lambda$ photoproduction measurements are made in this energy region the study should be of great detail and with high precision. Such an ambitious program is presently warranted only if the data can be obtained with more facility than has previously been possible.

ACKNOWLEDGMENTS

I am indebted to Professor P. Carruthers for his many suggestions and for his guidance throughout this work. I would also like to thank D. A. Edwards, F. von Hippel, and R. Reid for valuable discussions; and D. E. Groom, S. Mori, A. Sadoff, and N. Stanton for making available their experimental data prior to publication.

APPENDIX I

Kinematic Symbols

The masses, c.m. energies, and c.m. momenta of the interacting particles are defined as follows:

$$\text{proton } (M_p, E_p, -\mathbf{k}),$$
$$\text{photon } (0, k, \mathbf{k}),$$
$$K \text{ meson } (M_K, \omega, \mathbf{q}),$$
$$\Lambda\ (M_\Lambda, E_\Lambda, -\mathbf{q}).$$

In addition, M_Σ and M_{K^*} are the masses of the Σ and K^* (891) particles. The c.m. production angle of the K meson θ is given by

$$\mathbf{k}\cdot\mathbf{q}=kq\cos\theta,$$

where

$$k=|\mathbf{k}| \quad \text{and} \quad q=|\mathbf{q}|.$$

The laboratory photon energy E_γ is related to the total c.m. energy W by

$$W^2=M_p(2E_\gamma+M_p). \tag{A1}$$

TABLE III. Conversion between various kinematical quantities of the reactions $\gamma p \to K\Lambda$ and $\pi p \to K\Lambda$.

E_γ (lab) (GeV)	W (c.m.) (GeV)	q (c.m.) (GeV/c)	T_π (lab) (GeV)	p_π (lab) (GeV/c)
0.934	1.622	0.096	0.785	0.914
0.975	1.646	0.160	0.826	0.955
1.003	1.662	0.192	0.854	0.984
1.018	1.670	0.208	0.869	0.999
1.038	1.681	0.226	0.889	1.019
1.054	1.690	0.241	0.905	1.035
1.080	1.704	0.262	0.931	1.061
1.130	1.732	0.229	0.981	1.112
1.160	1.748	0.319	1.011	1.142
1.200	1.769	0.344	1.051	1.182
1.300	1.822	0.401	1.151	1.283
1.400	1.872	0.451	1.251	1.383

The usual four-momentum invariants are given by

$$\begin{aligned} s&=W^2,\\ t&=M_K{}^2-2k\omega+2kq\cos\theta,\\ u&=M_p{}^2+M_K{}^2-2E_p\omega-2kq\cos\theta. \end{aligned} \tag{A2}$$

Table III is a tabulation of the numerical values of the conversions between E_γ, W, q, T_π, and p_π for values of E_γ for which there exist experimental data. Laboratory pion kinetic energy and momentum which, when a pion is incident on a proton lead to the same total energy W, are designated by T_π and p_π.

Center-of-Mass Cross Section and Polarization

The cross section is given by[59]

$$\frac{d\sigma}{d\Omega}=\frac{q}{k}|\langle\chi_f|F|\chi_i\rangle|^2, \tag{A3}$$

where χ_i, χ_f are initial and final Pauli spinors and

$$\begin{aligned} F=&F_1(\sigma\cdot\hat{\epsilon})+F_2(i\boldsymbol{\sigma}\cdot\hat{q}\boldsymbol{\sigma}\cdot\hat{\epsilon}\times\hat{k})\\ &+F_3(\boldsymbol{\sigma}\cdot\hat{k}\hat{q}\cdot\hat{\epsilon})+F_4(\boldsymbol{\sigma}\cdot\hat{q}\,\hat{q}\cdot\hat{\epsilon}). \end{aligned} \tag{A4}$$

Here, $\boldsymbol{\sigma}$ is the Pauli spin operator and $\hat{\epsilon}$ is the photon polarization vector. The F_i's are independent of initial and final spin states.

For unpolarized initial states

$$\begin{aligned} d\sigma/d\Omega=&(q/k)\mathrm{Re}\{|F_1|^2+|F_2|^2-(2\cos\theta)F_1{}^*F_2\\ &+(\sin^2\theta)[\tfrac{1}{2}|F_3|^2+\tfrac{1}{2}|F_4|^2\\ &+F_1{}^*F_4+F_2{}^*F_3+(\cos\theta)F_3{}^*F_4]\} \end{aligned} \tag{A5}$$

and the Λ polarization in the direction of $\hat{k}\times\hat{q}$ is given by

$$\begin{aligned} \mathbf{P}_{\Lambda(\hat{k}\times\hat{q})}d\sigma/d\Omega=&(q/k)(\sin\theta)\\ &\times\mathrm{Im}[-2F_1{}^*F_2-F_1{}^*F_3+F_2{}^*F_4\\ &+(\sin^2\theta)F_3{}^*F_4+(\cos\theta)(F_2{}^*F_3-F_1{}^*F_4)]. \end{aligned}$$

The F_i's are related to the invariant amplitudes A_j of the T matrix, where

$$T=\sum_j A_j\bar{u}(p_2)M_ju(p_1),$$

and

$$\begin{aligned} M_1&=-\gamma_5\gamma\cdot\epsilon\gamma\cdot k,\\ M_2&=2\gamma_5(\epsilon\cdot p_1k\cdot p_2-\epsilon\cdot p_2k\cdot p_1),\\ M_3&=\gamma_5(\gamma\cdot\epsilon k\cdot p_1-\gamma\cdot ke\cdot p_1),\\ M_4&=\gamma_5(\gamma\cdot\epsilon k\cdot p_2-\gamma\cdot ke\cdot p_2). \end{aligned} \tag{A6}$$

[59] The results of Appendix I have been derived and stated in many references; they are listed here only for consistency. Most of the expressions were initially given in CGLN (Ref. 35). The equations as given here closely follow the more detailed deviation of Gourdin and Dufour (Ref. 2). The metric and definitions of the γ matrices are that of J. D. Bjorken and S. D. Drell, *Relativistic Quantum Mechanics* (McGraw-Hill Book Company, Inc., New York, 1964).

The M_j are Lorentz- and gauge-invariant quantities; k, p_1, and p_2 are the four-momenta of the photon, proton, and Λ; ϵ is the polarization four-vector; u and $\bar{u}$ are the appropriate Dirac spinors.

Using the above invariants, we have

$$F_1=\frac{k}{4\pi}\left(\frac{E_\Lambda+M_\Lambda}{2W}\right)^{1/2}\left[A_1-\frac{W+M_p}{2}A_3-\frac{k_\mu p_2{}^\mu}{W-M_p}A_4\right],$$

$$F_2=\frac{k}{4\pi}\left(\frac{E_\Lambda-M_\Lambda}{2W}\right)^{1/2}\left[-A_1-\frac{W-M_p}{2}A_3-\frac{k_\mu p_2{}^\mu}{W+M_p}A_4\right],$$

$$F_3=\frac{kq}{4\pi}\left(\frac{E_\Lambda+M_\Lambda}{2W}\right)^{1/2}[-(W-M_p)A_2+A_4], \tag{A7}$$

$$F_4=\frac{kq}{4\pi}\left(\frac{E_\Lambda-M_\Lambda}{2W}\right)^{1/2}[(W+M_p)A_2+A_4],$$

where

$$k_\mu p_2{}^\mu=-\tfrac{1}{2}(u+M_\Lambda{}^2).$$

Born Amplitudes

The amplitudes A_i resulting from the diagrams of Fig. 1 are evaluated using the following vertex factors:

$$\begin{aligned}
&(\gamma pp) && e\gamma\cdot\epsilon+\mu_p\gamma\cdot k\gamma\cdot\epsilon \quad (\mu_p=e\kappa_p/2M_p),\\
&(K^+p\Lambda) && ig_{K\Lambda N}\gamma_5,\\
&(K^+p\Sigma) && ig_{K\Sigma N}\gamma_5,\\
&(\gamma K^+K^+) && e\epsilon\cdot(2q-k),\\
&(\gamma\Lambda\Lambda) && \mu_\Lambda\gamma\cdot k\gamma\cdot\epsilon, \quad (\mu_\Lambda=e\kappa_\Lambda/2M_\Lambda),\\
&(\gamma\Lambda\Sigma) && \mu_T\gamma\cdot k\gamma\cdot\epsilon \quad [\mu_T=e\kappa_T/(M_\Lambda+M_\Sigma)],\\
&(\gamma K^{*+}K^+) && (g_{K^*K\gamma}/m)\epsilon^{\mu\nu\rho\sigma}\epsilon_\nu k_\rho r_\sigma,\\
&(K^{*+}p\Lambda) && g^V{}_{K^*\Lambda N}\gamma^\mu+[g^T{}_{K^*\Lambda N}/(M_p+M_\Lambda)]\gamma\cdot r\gamma^\mu,
\end{aligned} \tag{A8}$$

where r^σ is the four-momentum of the exchanged vector meson ($r^\sigma=p_2{}^\sigma-p_1{}^\sigma$) and m is an arbitrary mass chosen to make $g_{K^*K\gamma}$ dimensionless. We have used $m=1.0$ GeV in the evaluation of the G_V and G_T couplings. The constant $g_{K^*K\gamma}$ is related to the $K^{*+}\to K^++\gamma$ decay width by

$$\begin{aligned}
\Gamma_{K^{*+}\to K^+\gamma}&=\frac{1}{3}\frac{g_{K^*K\gamma}{}^2}{4\pi m^2}p_K{}^3\\
&=\frac{1}{24}\frac{g_{K^*K\gamma}{}^2}{4\pi m^2}[M_{K^*}(1-M_K{}^2/M_{K^*}{}^2)]^3\\
&=9.8\ \text{MeV}\,g_{K^*K\gamma}{}^2/4\pi.
\end{aligned} \tag{A9}$$

The A_i amplitudes are

$$\begin{aligned}
A_1=&\frac{g_\Lambda e}{s-M_p{}^2}(1+\kappa_p)+\frac{g_\Lambda e}{u-M_\Lambda{}^2}\kappa_\Lambda+\frac{G_\Sigma e}{u-M_\Sigma{}^2}\\
&+\frac{G_V}{m}\frac{(M_\Lambda+M_p)}{(t-M_{K^*}{}^2)}+\frac{G_T t}{m(M_p+M_\Lambda)}\frac{1}{(t-M_{K^*}{}^2)},\\
A_2=&\frac{2g_\Lambda e}{(t-M_K{}^2)(s-M_p{}^2)}+\frac{G_T}{m(M_p+M_\Lambda)}\frac{1}{(t-M_{K^*}{}^2)},\\
A_3=&\frac{g_\Lambda e}{(s-M_p{}^2)}\frac{\kappa_p}{M_p}+\frac{G_V}{m}\frac{1}{(t-M_{K^*}{}^2)}\\
&-\frac{G_T}{m(M_p+M_\Lambda)}\frac{(M_\Lambda-M_p)}{(t-M_{K^*}{}^2)},\\
A_4=&\frac{g_\Lambda e}{(u-M_\Lambda{}^2)}\frac{\kappa_\Lambda}{M_\Lambda}+\frac{G_\Sigma e}{(u-M_\Sigma{}^2)}\frac{2}{(M_\Lambda+M_\Sigma)}\\
&+\frac{G_V}{m}\frac{1}{(t-M_{K^*}{}^2)}+\frac{G_T}{m}\frac{(M_\Lambda-M_p)}{(M_\Lambda+M_p)}\frac{1}{(t-M_{K^*}{}^2)},
\end{aligned} \tag{A10}$$

where

$$\kappa_p=1.79,\quad \kappa_\Lambda=-1.00,\quad e^2/4\pi=1/137,$$

and G_Σ, G_V, G_T are defined by Eq. (1).

Multipole Partial-Wave Expansion and Decomposition of the F_i Amplitudes

The F_i amplitudes are related to the partial-wave amplitudes $M_{l\pm}$ and $E_{l\pm}$. Both the expressions for the F_i as functions of $M_{l\pm}$ and $E_{l\pm}$, and the inverse relations have been given, for example, by Ball,[60] and will not be displayed here. The contribution to the integral cross section from any of the various $M_{l\pm}$ or $E_{l\pm}$ is

$$\sigma(M_{l\pm},E_{l\pm})=4\pi\frac{q}{k}\frac{J+\frac{1}{2}}{2}j_\gamma(j_\gamma+1)\times\{|M_{l\pm}|^2,|E_{l\pm}|^2\}, \tag{A11}$$

where

$$\begin{aligned}
j_\gamma&=l \quad \text{for} \quad M_{l\pm},\\
j_\gamma&=l\pm1 \quad \text{for} \quad E_{l\pm}.
\end{aligned}$$

Barrier Penetration Factors

The barrier penetration factors $v_l(qR)$ given by Blatt and Weisskopf[27] are

$$\begin{aligned}
&v_0(x)=1,\\
&v_1(x)=x^2/(1+x^2),\\
&v_2(x)=x^4/(9+3x^2+x^4),\\
&v_3(x)=x^6/(225+45x^2+6x^4+x^6),
\end{aligned} \tag{A12}$$

where

$$x=qR,$$

and $1/R=200$ MeV has been used in these calculations.

[60] J. S. Ball, Phys. Rev. **124**, 2014 (1961); Eqs. (3.8)–(3.15). The $\mathfrak{F}_i$ of his paper are identical with our F_i.

APPENDIX II

Experimental Data

Tables IV and V are a tabulation of the existing low energy experimental data.[61] Data published prior to 1962 are not included.[62] The data as shown represent the final results of the various experimenters whereas in some cases the references quoted give preliminary results.[63] Some of the data have not been used in our χ^2 analysis and are so indicated.

TABLE IV. Differential cross-section data for the reaction $\gamma+p \rightarrow K+\Lambda$.

E_γ nominal (MeV)	E_γ (MeV)	$\theta^K_{\text{c.m.}}$ (deg)	$d\sigma/d\Omega$ (10^{-31}cm^2/sr)	Ref.
934[a]	934	90.0	0.55±0.04	9
942[b]	942	60.0	0.67±0.06	25
964[b]	964	54.0	0.93±0.06	25
975	976	31.1	1.34±0.08	9
	974	64.0	1.33±0.08	9
1003	1002	30.0	2.04±0.07	9
	1003	60.3	1.69±0.09	9
	1004	88.6	1.54±0.09	9
	1004	132.0	1.21±0.10	9
1018	1013	30.3	2.28±0.11	9
	1020	43.6	1.96±0.11	9
	1018	55.6	2.00±0.10	9
	1022	69.8	1.55±0.08	9
	1024	94.2	1.45±0.11	9
	1018	97.0	1.33±0.06	9
1038	1040	27.5	2.81±0.14	9
	1036	45.0	2.30±0.08	9
1054	1054	30.0	2.76±0.15	9
	1054	31.0	2.84±0.22	10
	1055	42.5	2.71±0.13	9
	1054	48.0	2.33±0.19	10
	1054	53.5	2.44±0.14	9
	1051	80.2	1.96±0.12	9
	1054	89.7	1.57±0.09	9
	1060	132.3	1.23±0.11	9
1080	1080	46.5	2.44±0.12	9
	1080	46.5	2.79±0.18	10
	1080	90.0	1.58±0.08	9
	1080	119.7	1.25±0.08	9
1100[b]	1100	89.9	1.39±0.09	16
1130	1130	90.0	1.42±0.13	9
1160	1160	36.0	2.59±0.17	11
	1160	60.0	2.06±0.12	11
	1160	75.0	2.05±0.16	11
	1160	90.0	1.44±0.10	11
	1160	135.0	0.79±0.09	11
1200	1200	15.0	3.79±0.27	10
	1200	25.0	3.34±0.15	10
	1200	30.0	3.41±0.19	10
	1200	35.0	3.00±0.14	10
	1200	42.0	2.84±0.15	10
	1200	49.0	2.82±0.16	10
	1200	55.0	2.76±0.16	10
	1200	63.0	2.14±0.16	10
	1200	70.0	2.02±0.14	10
	1200	78.0	1.94±0.17	10
	1200	85.0	1.54±0.18	10
	1200	90.0	1.52±0.12	11
	1200[b]	90.2	1.43±0.07	16
	1200	127.0	1.34±0.40	10
1300[b]	1300	89.8	1.43±0.09	16
1400[b]	1400	17.5	2.79±0.24	11
	1400	25.0	2.71±0.21	11
	1400	32.5	2.94±0.21	11
	1400	40.0	2.61±0.14	11
	1400	45.0	2.66±0.16	11
	1400	60.0	2.32±0.11	11
	1400	75.0	1.81±0.13	11
	1400	90.0	1.57±0.08	11
	1400	142.5	1.17±0.10	11

[a] Experimental error increased to $\pm 0.12 \times 10^{-31}$ cm^2/sr in the χ^2 calculations.
[b] Not used in χ^2 analysis. (Not available at the time the calculations were performed.)

TABLE V. The Λ polarization data and the interpolated data used in the χ^2 analysis (see Sec. III). The $(\hat{k}\times\hat{q})$ indicates only the direction in which the polarization vector has been defined. The polarization values given here are for a decay asymmetry parameter α given by $\alpha=0.62\pm0.07$.[a] The errors indicated are only statistical.

Experimental data				Interpolated data		
E_γ (MeV)	$\theta^K_{\text{c.m.}}$ (deg)	$\mathbf{P}(\hat{k}\times\hat{q})$	Ref.	E_γ (MeV)	$\theta^K_{\text{c.m.}}$ (deg)	$\mathbf{P}(\hat{k}\times\hat{q})$
963	91	−0.19±0.14	15	975	90	−0.15±0.12
1000	93	−0.23±0.11	14	1003	90	−0.23±0.11
1018	92	−0.30±0.13	15	1018	90	−0.20±0.10
1026	87	−0.21±0.10	14			
1020	61	−0.16±0.12	15			
1050	85	−0.39±0.15	15	1054	90	−0.40±0.10
1056	80	−0.38±0.09	14			
1095	91	−0.09±0.11	14	1080	90	−0.28±0.10
1100	90	−0.34±0.09	16			
1121	90	−0.37±0.11	14	1130	90	−0.37±0.11
1200	90	−0.30±0.07	16	1200	90	−0.31±0.07
1300	90	−0.08±0.07	16	1300	90	−0.08±0.07

[a] J. W. Cronin and O. E. Overseth, Phys. Rev. **129**, 1795 (1963).

[61] High-energy measurements have been made by V. B. Elings *et al.*, Phys. Rev. Letters **16**, 474 (1966).
[62] The early Cornell data have possible systematic errors which make them difficult to compare with the later data. Early California Institute of Technology data have large statistical errors.
[63] D. E. Groom, S. Mori, A. Sadoff, and N. Stanton (private communication).